BULLETIN OF THE CHEMICAL SOCIETY OF JAPAN, VOL. 50 (4), 810—816 (1977)

Heat Capacity of Potassium *p*-Chloranil Anion Radical Salt between 13 and 330 K*

Akio Kosaki,† Michio Sorai, Hiroshi Suga, and Syûzô Seki

Department of Chemistry, Faculty of Science, Osaka University, Toyonaka, Osaka 560

(Received October 18, 1976)

The heat capacity measurement for an organic free-radical salt, potassium *p*-chloranil, revealed a first-order phase transition at $T_c=260.01$ K. In spite of a first-order nature, the pre- and the post-transitional effects are remarkable. The enthalpy and the entropy of transition were determined to be $\Delta H=2796$ J mol^{-1} and $\Delta S=11.06$ JK^{-1} mol^{-1}, respectively. The magnetic contribution to ΔS is only 2.23 JK^{-1} mol^{-1} when a dimeric configuration with a singlet-triplet spin equilibrium is assumed in the low temperature phase and a monomeric behavior of radicals with spin doublet is assumed above T_c. The present phase transition bears a close resemblance to a spin-Peierls transition in a linear chain system. The infrared spectrum at 120 K indicates a possible formation of dimers in the low temperature phase of this salt. A phenomenological model for the present phase transition is presented.

Among a number of stable organic free radicals, the compounds which exhibit a cooperative phase transition due to unpaired electrons are very scarce. Moreover, these phase transitions are quite unique in that the spin and electronic state and the structural change are inseparably related to one another and that the mechanism of phase transition is different from radical to radical.

In this paper we report the heat capacity of potassium *p*-chloranil crystal [abbreviated hereafter as $K^+(p\text{-chloranil})^{\dot{-}}$ or more simply as $K^+(CA)^{\dot{-}}$]. This is one of the typical anion radical salts together with the TCNQ salts. The magnetic susceptibility and the electron paramagnetic resonance (EPR) measured by Andre *et al.*[1] revealed a first-order phase transition at $T_c=260$ K on raising and at $T_c=210$ K on lowering temperature. The magnetic susceptibility above T_c follows well the Curie-Weiss law while the magnetic behavior below T_c is described by the energy scheme of a singlet-triplet equilibrium. This result suggests that the *p*-chloranil anion radicals exist as monomers in the $K^+(CA)^{\dot{-}}$ salt above T_c and as dimers below T_c. EPR,[1,2] electronic absorption spectra,[3-6] and X-ray diffraction analysis[7] of this salt support the monomeric behavior of the *p*-chloranil anion radicals in the high temperature phase. On the other hand, Hiroma and Kuroda[8] investigated the temperature dependence of the electronic absorption spectra of the $K^+(CA)^{\dot{-}}$ salt and found that an abrupt increase of intensity occurs in the charge-transfer band at the phase transition point when the specimen is cooled. This fact suggests that the low temperature phase has a crystal structure of a dimeric arrangement of the *p*-chloranil anions. Although an X-ray diffraction analysis of the low temperature phase has not been made, this suggestion seems to be quite reasonable in comparison with the electronic absorption spectra of $K^+(CA)^{\dot{-}}$ in solution,[5,6,9,10] where the monomer-dimer equilibrium is established.

In spite of a useful method which provides important information concerning the energetic aspects, the number of works in which heat capacity measurements are applied to organic free-radical salts are scarce.[11-21] The present paper clearly reveals a first-order phase transition at 260.01 K. As is in the case of other radicals, the magnetic contribution to the transition entropy is not dominant. Although a quantitative explanation for the phase transition is not given, a phenomenological model is described here.

Infrared spectroscopy also serves as a useful tool to elucidate the local symmetry of the constituent entity. But the infrared spectra hitherto reported are room temperature data.[22-24] We also report here the infrared spectra of the $K^+(CA)^{\dot{-}}$ salt between 4000 and 30 cm^{-1} in both the high and the low temperature phases.

Experimental

Material. The starting materials, potassium iodide and *p*-chloranil, were recrystallized twice from water and benzene, respectively. The solvent, acetone, was purified by the method of Scheibe *et al.*[25] The $K^+(CA)^{\dot{-}}$ salt was prepared according to the method of Torrey and Hunter.[26] The reaction temperature was 263±2 K. The product was washed with chilled acetone and dried *in vacuo* for three days. Found: C, 25.26; Cl, 49.37%. Calcd for $C_6Cl_4O_2K$: C, 25.29; Cl, 49.76%.

It has been reported[7,8,10] that the preparation method by Torrey and Hunter does not yield one and the same modification of the $K^+(CA)^{\dot{-}}$ crystal. We prepared the $K^+(CA)^{\dot{-}}$ salt at two different temperatures (263 and 273 K) and examined their thermal properties by using a differential scanning calorimeter (DSC). The salt prepared at 263 K exhibited a sharp endothermic peak due to the phase transition at 260 K while the salt precipitated above 273 K gave a broad peak. This fact implies the contamination of some impurities in the salt prepared above 273 K. On the other hand, it is possible that the salt prepared at 263 K would be a mixture of the high and the low temperature modifications as the synthesis temperature is close to the phase transition point ($T_C=260.01$ K) and thus the free energies of both phases are virtually the same magnitude in this temperature region. In fact the DSC curve showed the trace of a small amount of the low temperature modification. Therefore, whenever the infrared and the Raman spectra were recorded at roon temperature, the specimen was once cooled down to about 100 K and warmed up to a room temperature.

Heat Capacity Measurement. The heat capacity was measured with an adiabatic calorimeter[27] in the temperature

---

* Presented before the Symposium on the Magnetochemistry, Nagoya (1970).

† Deceased on July 16, 1974.

region from 13 to 330 K. The sample of 8.0239 g (=0.028156 mol) was sealed into the calorimeter cell together with a small amount of helium gas as the heat exchanger.

Infrared and Raman Spectra. The infrared spectra at a room temperature and 120 K were recorded on a Grating-type Infrared Spectrophotometer Model DS-402G (Japan Spectroscopic Co., Ltd.) in the wave number region from 4000 to 400 cm^{-1} and on a Spectrophotometer Model FIS-001 (Hitachi Ltd.) in the range from 400 to 30 cm^{-1}. Nujol mull method was employed for the preparation of samples.

The Raman spectra of $K^+(CA)^{\cdot-}$ salt were recorded on a laser Raman Spectrophotometer Model R-750 with the argon laser (514.5 nm) in the range from 0 to 4000 cm^{-1} at a room temperature. It was difficult to obtain a good Raman spectrum of this salt because of its continuous absorption band in the corresponding wave number region and the instability of this radical salt against the strong argon laser exposure.

Results

Heat Capacity of $K^+(CA)^{\cdot-}$ Salt. Prior to the heat capacity measurement, we performed the DSC measurement for the $K^+(CA)^{\cdot-}$ salt. An exothermic peak was observed at 220 K on cooling and an endothermic peak appeared at 260 K in a heating run. A large hysteresis effect with a temperature interval of 40 K indicates a typical first-order nature of the phase transition.

The measured values for the heat capacity are plotted in Fig. 1 and the numerical values are given in Table 1. The standard thermodynamic functions for the $K^+(CA)^{\cdot-}$ salt are shown in Table 2. A sharp heat capacity anomaly is found around 260 K. The phase transition

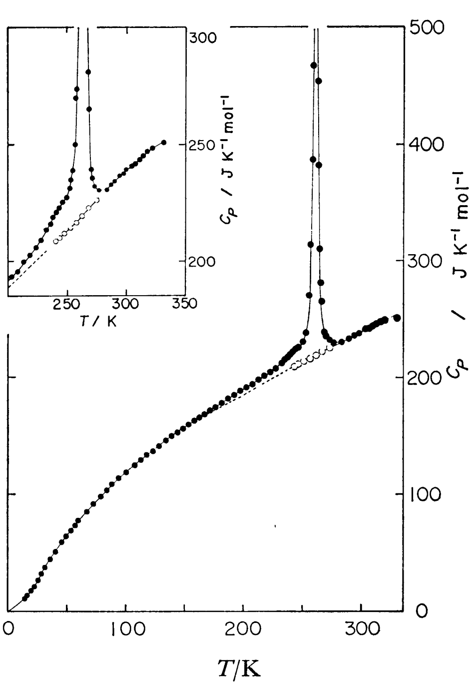

Fig. 1. The molar heat capacity of the $K^+(p\text{-chloranil})^{\cdot-}$ anion radical salt. Open circles indicate the heat capacities of the supercooled high temperature phase. Broken line is the extrapolated curve of the supercooled high temperature phase and serves as a "normal" heat capacity for the estimation of the transition enthalpy and entropy.

Table 1. Heat capacity of $K^+(p\text{-chloranil})^{\cdot-}$

T / K	C_p / JK^{-1} mol^{-1}	T / K	C_p / JK^{-1} mol^{-1}	T / K	C_p / JK^{-1} mol^{-1}	T / K	C_p / JK^{-1} mol^{-1}	T / K	C_p / JK^{-1} mol^{-1}
13.81	11.57	90.68	111.76	175.92	171.89	247.13	229.28	281.45	229.36
14.81	12.63	93.66	114.73	178.66	177.67	248.94	231.29	282.75	230.13
16.06	14.24	96.59	117.41	181.32	179.35	250.15	232.25	282.90	230.96
17.41	15.80	99.92	120.15	183.92	180.86	250.65	233.08	283.24	230.76
18.80	17.91	103.66	123.43	186.56	183.18	252.54	237.31	283.89	230.85
20.21	19.80	106.87	125.90	189.19	183.83	253.73	240.85	285.16	232.05
21.63	21.43	109.58	128.43	191.81	186.24	254.91	251.65	285.88	233.36
23.06	24.27	112.25	130.39	194.43	188.11	255.31	272.02	286.70	234.25
24.53	27.24	114.89	132.50	197.03	189.72	256.07	273.53	287.11	233.68
25.98	29.94	117.50	134.98	199.61	191.19	256.98	315.92	288.22	235.25
27.46	32.72	120.08	137.48	202.18	192.85	257.17	341.36	289.78	234.28
29.00	35.31	122.63	138.31	204.74	194.43	258.30	389.02	290.32	233.69
30.83	38.30	125.16	140.79	207.29	195.54	258.79	469.58	290.67	234.91
32.96	41.58	127.66	143.41	209.83	197.58	259.25	528.99	291.73	235.13
35.10	45.13	130.15	144.72	212.36	199.52	259.80	621.16	292.47	236.98
37.22	48.72	133.80	147.41	214.88	200.69	260.53	639.39	292.72	235.16
39.46	51.51	136.23	149.40	217.39	202.37	261.37	548.82	294.00	236.58
42.05	54.67	138.65	151.13	219.89	204.76	262.28	455.88	296.27	238.51
45.05	59.16	141.05	152.89	222.40	205.90	263.26	383.63	297.58	238.85
48.73	64.17	143.43	154.18	224.91	207.65	264.30	311.74	298.55	239.43
52.76	69.67	145.83	155.57	227.38	209.01	265.40	281.97	300.83	239.94
56.45	73.80	148.19	157.83	227.92	211.76	266.52	265.68	302.70	242.17
59.88	78.09	150.54	159.16	230.79	213.59	270.30	234.60	303.11	239.10
63.11	82.37	152.86	160.94	233.64	216.22	272.52	232.11	305.39	241.23
66.18	85.75	155.17	162.46	234.73	216.53	273.39	228.46	306.12	244.50
69.12	88.97	157.47	164.23	237.15	219.09	276.27	230.05	307.67	242.14
72.16	92.70	159.75	165.22	239.29	221.63	276.30	229.44	309.95	244.61
75.32	95.86	162.02	166.82	239.57	221.64	276.59	229.94	312.59	247.19
78.37	99.55	164.27	169.08	241.98	224.10	277.09	230.74	316.36	248.35
81.18	102.31	166.52	169.80	242.10	224.28	279.61	230.53	320.12	249.12
83.48	104.64	168.75	171.40	244.38	226.51	280.17	231.52	328.54	248.60
85.41	106.43	170.98	173.06	244.71	225.69	281.05	231.54	330.79	251.31
87.77	108.95	173.19	174.51	246.76	228.63	281.19	229.14		
			Supercooled Phase						
242.91	210.89	255.36	216.44	261.78	220.37	266.82	223.71	270.88	225.22
246.55	212.85	256.72	217.33	264.58	221.93	267.95	223.25	273.33	227.00
251.62	215.29	260.34	219.03						

Table 2. Standard thermodynamic functions of $K^+(p\text{-chloranil})^{\overline{\cdot}}$

T	$C_p°$	$S°$	$(H_T°-H_0°)/T$	$-(G_T°-H_0°)/T$
K	$J\,K^{-1}\,mol^{-1}$	$J\,K^{-1}\,mol^{-1}$	$J\,K^{-1}\,mol^{-1}$	$J\,K^{-1}\,mol^{-1}$
20	19.47	9.841	6.948	2.893
30	36.99	20.977	13.991	6.986
40	52.24	33.766	21.700	12.067
50	65.90	46.903	29.185	17.718
60	78.39	60.027	36.349	23.678
70	90.04	73.000	43.200	29.799
80	101.04	85.752	49.753	35.999
90	111.22	98.249	56.026	42.224
100	120.37	110.45	62.010	48.439
110	128.72	122.32	67.698	54.619
120	136.73	133.86	73.116	60.743
130	144.49	144.00	77.202	66.802
140	151.90	156.10	83.306	72.790
150	158.92	166.82	88.114	78.702
160	165.66	177.29	92.752	84.538
170	172.20	187.53	97.233	90.296
180	178.70	197.56	101.58	95.977
190	185.13	207.39	105.81	101.58
200	191.56	217.05	109.93	107.12
210	197.70	226.55	113.97	112.58
220	204.10	235.89	117.92	117.97
230	211.70	245.12	121.82	123.30
240	221.94	254.35	125.78	128.57
250	232.43	263.61	129.83	133.78
260	683.60	275.88	136.90	138.99
270	235.50	289.35	145.01	144.34
280	230.19	297.76	148.09	149.67
290	234.93	305.92	151.00	154.92
300	239.67	313.97	153.88	160.09
310	244.45	321.90	156.72	165.18

temperature T_c is determined to be 260.01 K. We succeeded in measuring the heat capacities for the supercooled high temperature phase between 240 and 270 K. These values are represented in Fig. 1 by open circles.

In order to determine the enthalpy and the entropy associated with the phase transition, it is necessary to separate the "excess" heat capacity from the total one by estimating a plausible "normal" heat capacity. In the present case, the normal heat capacity is rather easily determined by extrapolating the experimental values for the supercooled high temperature phase to the low temperature side. The broken line shown in Fig. 1 represents the normal heat capacity. In spite of the first-order nature of the present phase transition the excess heat capacity has its long tail down to about 150 K. This fact suggests a higher-order nature of the initial stage of the present phase transition. The enthalpy and the entropy of transition are determined to be $\Delta H = 2796\,J\,mol^{-1}$ and $\Delta S = 11.06\,J\,K^{-1}\,mol^{-1}$, respectively. The transition entropy corresponds to $R \ln 3.78$ and this value is too large to be accounted for solely in terms of the magnetic contribution.

According to the structural analysis by Konno *et al.*,[7] the $K^+(CA)^{\overline{\cdot}}$ salt has several polymorphs and two dominant modifications are denoted as the α-form (orthorhombic, space group $P2_12_12_1$ and molar volume $V_m = 139.3\,cm^3\,mol^{-1}$) and the β-form (orthorhombic, $P22_12$ and $V_m = 136.9\,cm^3\,mol^{-1}$). Hiroma and Kuroda[8] found that the amount ratio of the α- to the β-form is about 10: 1. As was described in the previous section, we found that when the synthesis temperature is higher than 273 K, the salt contains some impurities and when the salt is prepared at 263 K, the contamination of impurities is considerably reduced but a small amount of the crystals having the low temperature modification is mixed. In addition to this observation, the fact that the β-form has the slightly smaller molar volume than that of the α-form suggests that the β-form is the low temperature modification of the $K^+(CA)^{\overline{\cdot}}$ salt.

Temperature Dependence of Infrared Spectra. Figure 2 shows the infrared spectra of the $K^+(CA)^{\overline{\cdot}}$ salt at 295 and 120 K in the wave number region from 1800 to

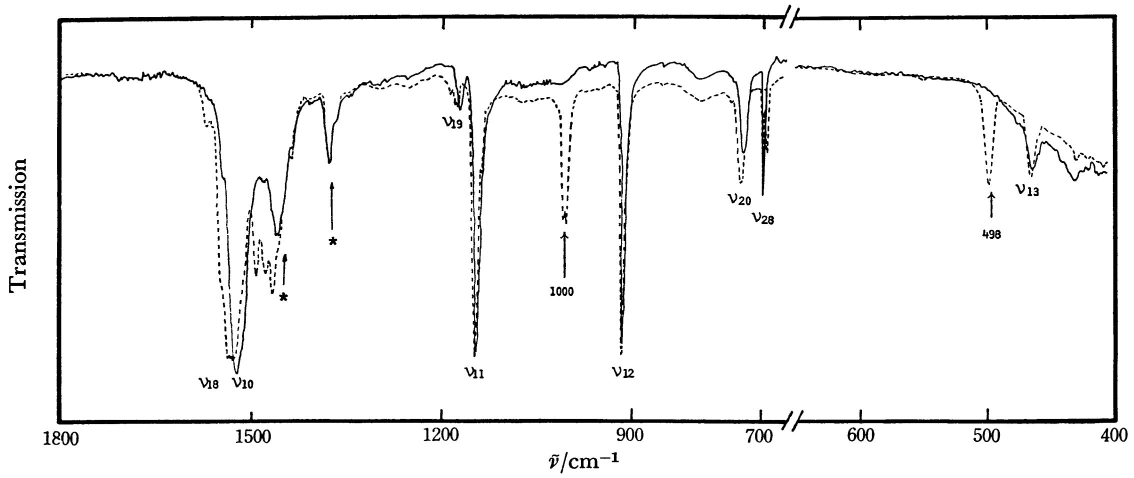

Fig. 2. Infrared spectra of the $K^+(CA)^{\overline{\cdot}}$ salt at 295 K (——) and at 120 K (-----). The bands marked with an asterisk are the absorption bands due to Nujol. In this and in Fig. 3, the fundamentals already assigned by Girlando *et al.*[24] are indicated by their symmetry species.

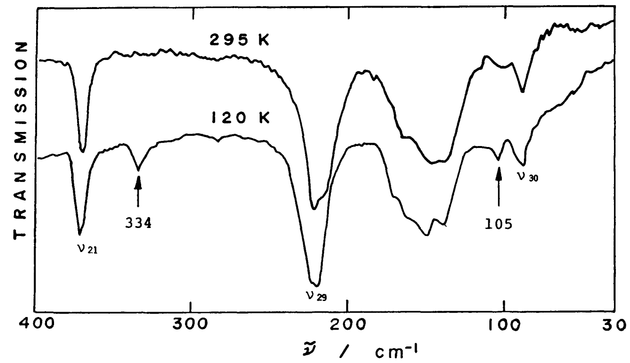

Fig. 3. Far infrared spectra of the $K^+(CA)^{\overline{\cdot}}$ salt at 295 and 120 K.

400 cm^{-1}. The far infrared spectra between 400 and 30 cm^{-1} are reproduced in Fig. 3. The spectra recorded at 295 K coincide well with the data previously reported.[23,24] The infrared spectra are markedly influenced by the effect of the phase transition. In the low temperature phase at 120 K, new absorption bands appear at 105, 334, 498, 1000 (doublet) and around 1450 cm^{-1} (doublet). Furthermore the band assigned as $b_{3u}\nu_{28}$ splits into a doublet.

Since the *p*-chloranil anion radical belongs to D_{2h} point group at least in the high temperature phase, it has a center of symmetry and a twofold axis. Under this symmetry the rule of mutual exclusion can be applied to the spectroscopic data. The gerade normal modes for the symmetry operation are infrared inactive and Raman active while the ungerade normal modes are infrared active and Raman inactive. The new bands at 1000, 498, and 334 cm^{-1} appeared in the low temperature phase seem to belong to the gerade normal modes in the high temperature phase because the Raman spectrum of this salt recorded at 295 K has the bands corresponding to the same wave numbers. Therefore, it is concluded that the D_{2h} symmetry of the *p*-chloranil anion radical in the high temperature phase is lowered in the low temperature phase through the intermolecular interaction characterized by the dimerization and/or by the variation of the crystalline field due to a possible structural change at the phase transition temperature. In this situation, some of the infrared inactive gerade modes are changed into the infrared active modes below the phase transition temperature.

Owing to the lower symmetry than D_{2h} of *p*-chloranil anion radical in the low temperature phase, there exist in general no multi-degenerate normal modes. Accordingly, the appearance of the doublets at 1000 and 698 cm^{-1} (the ν_{28} mode) should be attributed to two inequivalent anion radicals in the crystal lattice of the low temperature phase. Unfortunately the structural data on the low temperature phase of the $K^+(CA)^{\overline{\cdot}}$ radical salt, which confirms the present prediction, has not been reported. The *p*-chloranil anion radicals are known to behave as monomer in the high temperature phase and as dimer in the low temperature phase characterized by a siglet-triplet spin equilibrium.[8] This suggests a strong intermolecular interaction between adjacent radicals below the transition temperature. The selection rule of the infrared spectra in the low temperature phase is governed by the total symmetry of the dimeric entity. Two identical normal modes, which originally belong to two individual radicals forming a dimer, couple with each other and the absorption occurs at slightly different wave numbers. The origin of the seeming doublets at 1000 and 698 cm^{-1} can be interpreted in this way.

Hiroma and Kuroda[10] reported that the $K^+(CA)^{\overline{\cdot}}$ radical salt has a tendency to take water molecules into the crystal lattice when the crystal is exposed to a humid air. The hydrate is characterized by three infrared absorption bands at 3400 cm^{-1} (the O–H stretching), 1630 cm^{-1} (the H–O–H bending vibration) and 1000 cm^{-1} (the librational motion of water molecule). The present infrared spectra at 295 K show no bands at these wave number region, which indicates that the present salt is anhydrous.

Relationship between Magnetic Behavior and Phase Transition

Andre *et al.*[1] measured the magnetic susceptibility, χ, of the $K^+(CA)^{\overline{\cdot}}$ anion radical salt and concluded that the magnetic spins behave as in the singlet-triplet equilibrium below T_c while the magnetic behavior above T_c is accounted for in terms of spin doublet due to the monomeric radical. This prediction has been supported by various kinds of experiments such as EPR[1,2] electronic absorption spectra,[3–6,8] and the structural analysis.[7] However, the logic of Andre *et al.* leading to their conclusion is not correct in the meaning that they have drawn their conclusion based on their incorrect estimation of the asymptotic value of χT at infinite temperature for the singlet-triplet energy scheme. They obtained the value of $(\chi T)_\infty$ to be 1/4 and 3/8 for the singlet-triplet scheme (abbreviated as the ST-scheme) and the doublet scheme (the D-scheme), respectively. But in the present case, the value of $(\chi T)_\infty$ should be identical to each other.

The magnetic susceptibility for the ST-scheme is represented by

$$\chi = \left(\frac{N_A}{2}\right)\frac{S(S+1)g^2m_B{}^2}{3kT}\left\{1+\frac{1}{3}\exp\left(J/kT\right)\right\}^{-1} \quad (S=1), \quad (1)$$

where N_A is the Avogadro constant, g the electron g-factor $(=2.0)$, m_B the Bohr magneton, S the spin quantum number, and J the triplet excitation energy corresponding to the energy separation between the singlet and the triplet states. If the triplet density is defined by

$$\rho_T \equiv \left\{1+\frac{1}{3}\exp\left(J/kT\right)\right\}^{-1}, \quad (2)$$

we obtain the following relation:

$$\chi T = \frac{1}{2}\rho_T. \quad (3)$$

Because of $0 \leqq \rho_T \leqq 3/4$, the range of χT becomes

$$0\,(T=0) \leqq \chi T \leqq \frac{3}{8}\,(T=\infty). \quad (4)$$

On the other hand, the susceptibility for the D-scheme is given by the Curie law,

$$\chi = \frac{Ng^2 m_B^2}{3kT} S(S+1) \quad \left(S=\frac{1}{2}\right), \tag{5}$$

where N is the number of spins having $S=1/2$. Since the doublet density is defined by

$$\rho_D \equiv \frac{N_A}{N} \quad (0 \leqq \rho_D \leqq 1), \tag{6}$$

we obtain the following relations:

$$\chi T = \frac{3}{8}\rho_D \tag{7}$$

and

$$0(T=0) \leqq \chi T \leqq \frac{3}{8}(T=\infty). \tag{8}$$

We estimated the triplet excitation energy J and the doublet density ρ_D by applying respectively the ST- and the D-schemes to the magnetic susceptibility data obtained by Andre *et al.*[1] The results are shown in Fig. 4 in terms of J/k and ρ_D against T. It should be remarked here that the triplet excitation energy shows a constant value ($J/k=660$ K) below T_c. This fact supports the validity of the ST-scheme below T_c.

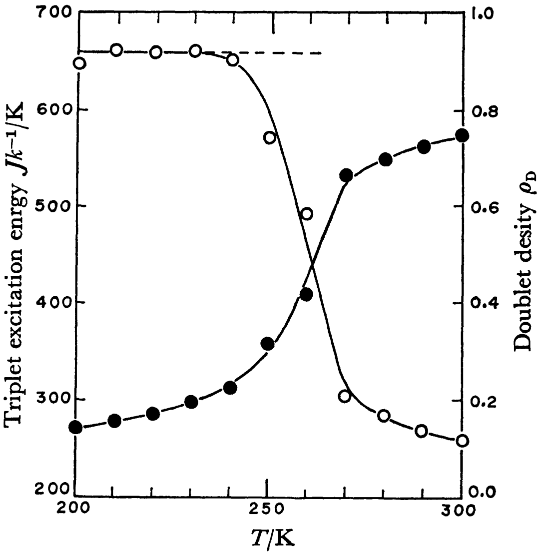

Fig. 4. The triplet excitation energy J/k(○) and the doublet density ρ_D(●) against temperature($T_C=260.01$ K) for the $K^+(CA)^{\overline{\cdot}}$ salt. These quantities are estimated from the magnetic susceptibility obtained by Andre *et al.*[1]

On the other hand, in the high temperature phase the magnetic feature is more complicated. If the doublet scheme is applied to the present system, the doublet density amounts to 0.75 at 300 K and shows a tendency to approach 1.00 with further increasing temperature. In case of the singlet-triplet scheme, the triplet excitation energy is considerably reduced to $J/k=250$ K at a room temperature. Although solely from the present result we cannot explicitly give an answer to the question of which scheme is established in the high temperature phase of the $K^+(CA)^{\overline{\cdot}}$ salt, it is very likely that most of the *p*-chloranil radicals behave as monomers with $S=1/2$ but the remaining minor fraction exists in the singlet-triplet equilibrium. With increasing temperature, the ST-scheme is transferred into the D-scheme. At any rate, the present phase transition is essentially characterized by the transition between dimer and monomer in a magnetic linear chain. This situation bears a close resemblance to a spin-Peierls transition in a Heisenberg linear chain system,[28] where an instability of magnetic linear chain at low temperatures is overcome by a structural phase transition coupled with the spin system.[29]

The entropy of the magnetic system with the triplet density ρ_T is represented by

$$S = \frac{1}{2}R\{\rho_T \ln 3 - \rho_T \ln \rho_T - (1-\rho_T)\ln(1-\rho_T)\}, \tag{9}$$

while the magnetic entropy due to the doublet density ρ_D is given by

$$S = R\rho_D \ln 2, \tag{10}$$

where R is the gas constant. We estimated the magnetic contribution to the transition entropy for the following three cases: (i) the ST-scheme below T_c and the D-scheme above T_c, (ii) the ST-scheme below and above T_c, and (iii) the D-scheme below and above T_c. As the pre- and the post-transitional effects are rather large in the heat capacity curve shown in Fig. 1, the estimation of the magnetic entropy has been made for the temperature interval between 200 and 285 K. In the case of (i), the change in spin state from the ST-scheme ($J/k=660$ K, $\rho_T=0.10$) to the D-scheme ($\rho_D=0.70$) yields the magnetic entropy of $\Delta S_{mag}=2.23$ J K^{-1} mol^{-1}. As to the case (ii), $\Delta S_{mag}=S(J/k=280$ K, $\rho_T=0.53) - S(J/k=660$ K, $\rho_T=0.10) = 3.49$ J K^{-1} mol^{-1}. The case (iii) gives the magnetic entropy of $\Delta S_{mag}=S(\rho_D=0.70)-S(\rho_D=0.14)=3.23$ J K^{-1} mol^{-1}. Since the total entropy arising from the phase transition is $\Delta S=11.06$ J K^{-1} mol^{-1}, the magnetic contribution corresponds merely to 20% for the case (i) and 30% for (ii) and (iii). The remaining entropy results from the phonon system. On the other hand, the total magnetic entropy for the $K^+(CA)^{\overline{\cdot}}$ salt is at most R ln 2 ($=5.76$ J K^{-1} mol^{-1}) independently of the spin scheme (see Eqs. 9 and 10), and the cooperative fraction of the magnetic entropy is 39, 61, and 56% for the cases (i), (ii), and (iii), respectively.

Phenomenological Model for Phase Transition

The phase transition found for the $K^+(CA)^{\overline{\cdot}}$ salt is of a first order in nature but the pre- and the post-transitional effects spread over a wide temperature region suggest easy fluctuations of the heterophases in this temperature region. We apply here a phenomenological model, which is virtually the same with the Frenkel theory of heterophase fluctuation in liquid,[30] to the present phase transition.

We shall assume that one phase contains "embryos" of a second phase in the transition region and that each embryo consists of a uniform size. We consider a system consisting of N cells each of which contains n molecules. The product of N and n is equated to Avogadro's constant N_A. The interaction energy between the adjacent cells belonging to the low and the high temperature phases is denoted by J_{LH}. As the surface area of a cell changes with its dimension, the interaction energy is multiplied by $N^{1/3}$. The Gibbs energy of the system can be written as

$$G = G_\mathrm{L}x + G_\mathrm{H}(1-x) + N^{1/3}J_\mathrm{LH}x(1-x) + NkT\{x\ln x + (1-x)\ln(1-x)\}, \tag{11}$$

where G_L and G_H are the Gibbs energies of the low and the high temperature phases, respectively, and x is the fraction of the cells belonging to the low temperature phase. The equilibrium value of x may be found by minimizing G with respect to x: $\partial G/\partial x=0$. The solution to this is given by those values of x which satisfy

$$\frac{1}{x} = 1 + \exp[\{G_\mathrm{L}-G_\mathrm{H}+N^{1/3}J_\mathrm{LH}(1-2x)\}/NkT]. \tag{12}$$

The heat capacity of the system, C_p, is represented as follows:

$$C_p = xC_{p\mathrm{L}} + (1-x)C_{p\mathrm{H}} + \left(\frac{\partial x}{\partial T}\right)\{H_\mathrm{L}-H_\mathrm{H}+N^{1/3}J_\mathrm{LH}(1-2x)\}, \tag{13}$$

here

$$\left(\frac{\partial x}{\partial T}\right)\frac{N^{2/3}x(1-x)}{N^{2/3}kT-2J_\mathrm{LH}x(1-x)}\left(\frac{S_\mathrm{H}-S_\mathrm{L}}{N}+k\ln\frac{x}{1-x}\right) \tag{14}$$

where H and S mean the enthalpy and the entropy of the system. When the denominator of Eq. 14 becomes zero, the heat capacity (Eq. 13) diverges infinitely at T_c. According to its definition, the J_LH is positive. Therefore, the condition under which a phase transition occurs is given by

$$J_\mathrm{LH}/N^{2/3} \geqq 2kT_\mathrm{C}. \tag{15}$$

When $(J_\mathrm{LH}/N^{2/3})$ is equal to $2kT_\mathrm{c}$, the phase transition is of a second order while in case of $(J_\mathrm{LH}/N^{2/3})>2kT_\mathrm{c}$ a first-order phase transition takes place. If we define f as a fraction of the transition enthalpy corresponding to the first-order phase transition, namely the latent heat, the following relationship is obtained:

$$f^2 = 1 - 2kT_\mathrm{C}N^{2/3}/J_\mathrm{LH}. \tag{16}$$

The fraction of the latent heat increases with increasing the value of $(J_\mathrm{LH}/N^{2/3})$. On the other hand, when J_LH is constant, the anomalous heat capacity due to the phase transition becomes broad with increasing N.

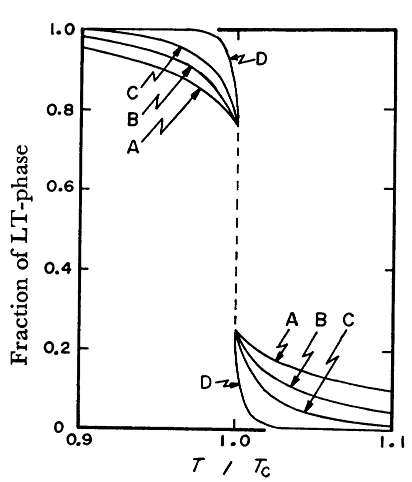

Fig. 5. Temperature dependence of the fraction of the low temperature phase, x, under a condition of $(J_\mathrm{LH}/N^{2/3})=2.2kT_\mathrm{C}$. $N_\mathrm{A}/N=5$(A), 10(B), 20(C), and 100 (D).

In order to apply this model to the actual system, the hypothetical Gibbs energies of both the low and the high temperature phases are necessary. We estimated these energies by extrapolating the heat capacity curve of the $\mathrm{K^+(CA)^{\dot{-}}}$ salt above and below T_c. Figure 5 demonstrates temperature dependences of the fraction of the low temperature phase, x, for four different values of N_A/N under a condition of $(J_\mathrm{LH}/N^{2/3})=2.2\,kT_\mathrm{c}$. A discontinuity of x at T_c is apparent.

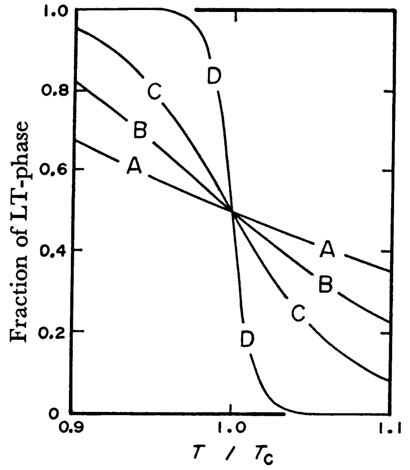

Fig. 6. Temperature dependence of the fraction of the low temperature phase, x, under a condition of $(J_\mathrm{LH}/N^{2/3})=0$.
$N_\mathrm{A}/N=5$(A), 10(B), 20(C), and 100(D).

When $(J_\mathrm{LH}/N^{2/3})$ is smaller than $2kT_\mathrm{c}$, the present model gives rise to neither a first- nor a second-order phase transition. This situation is illustrated in Fig. 6. The gradient of x at T_c increases with decreasing N.

The "best" fit of the calculated values to the experimental one is shown in Fig. 7. Here, the experimental value of x has been determined as $x=\Delta H(T)/\Delta H$. Although the phase transition of the $\mathrm{K^+(CA)^{\dot{-}}}$ salt is of a typical first order, the "best" fit between the

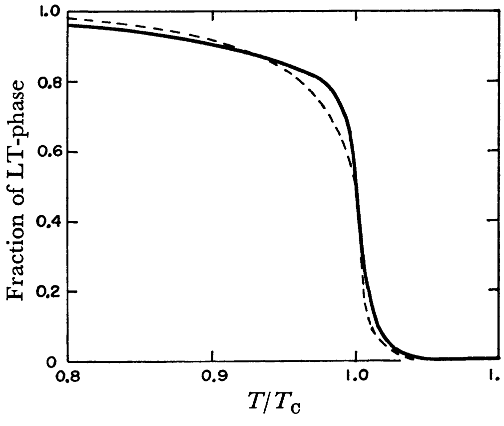

Fig. 7. Comparison of the fraction of the low temperature phase, x, between the experiment and the theory.
Solid line: the experimental curve.
Broken line: $(J_\mathrm{LH}/N^{2/3})=1.8kT_\mathrm{C}$, $N_\mathrm{A}/N=5(T<T_\mathrm{C})$ and $200(T>T_\mathrm{C})$.

experiment and the present model is obtained under a condition of $(J_{\mathrm{LH}}/N^{2/3})=1.8\,kT_{\mathrm{c}}$. This fact indicates a complexity of the phase transition found for organic free radical salts as well as an incompleteness of the present model. However, it is interesting to note that the number of radicals included in a cell varies from $N_{\mathrm{A}}/N=5$ in the low temperature phase to 200 in the high temperature phase. This suggests a considerably different correlation between radicals below and above T_{c}.

References

1) J. J. Andre, J. Clementz, R. Jesser, and G. Weill, *C. R. Acad. Sci., Ser. B*, **266**, 1057 (1968).

2) R. J. Faber and M. P. Faber, *J. Chem. Phys.*, **39**, 3541 (1963).

3) J. J. Andre and G. Weill, *C. R. Acad. Sci., Ser. B*, **269**, 499 (1969).

4) Y. Iida, *Bull. Chem. Soc. Jpn.*, **43**, 2772 (1970).

5) N. Sakai, I. Shirotani, and S. Minomura, *Bull. Chem. Soc. Jpn.*, **44**, 675 (1971).

6) J. J. Andre and G. Weill, *Chem. Phys. Lett.*, **9**, 27 (1971).

7) M. Konno, H. Kobayashi, F. Marumo, and Y. Saito, *Bull. Chem. Soc. Jpn.*, **46**, 1987 (1973).

8) S. Hiroma and H. Kuroda, *Bull. Chem. Soc. Jpn.*, **46**, 3645 (1973).

9) J. J. Andre and G. Weill, *Mol. Phys.*, **15**, 97 (1968).

10) S. Hiroma and H. Kuroda, *Bull. Chem. Soc. Jpn.*, **47**, 3014 (1974).

11) J. P. Goldsborough, M. Mandel, and G. E. Pake, "Proceedings of the VII-th International Conference on Low Temperature Physics," ed by G. M. Graham and A. C. H. Hallett, University of Toronto Press, Toronto (1961), p. 702.

12) W. O. Hamilton and G. E. Pake, *J. Chem. Phys.*, **39**, 2694 (1963).

13) H. Chihara, M. Nakamura, and S. Seki, *Bull. Chem. Soc. Jpn.*, **38**, 1776 (1965).

14) H. Lemaire, P. Rey, A. Rassat, A. Combarieu, and J. C. Michel, *Mol. Phys.*, **14**, 201 (1968).

15) A. Kosaki, H. Suga, S. Seki, K. Mukai, and Y. Deguchi, *Bull. Chem. Soc. Jpn.*, **42**, 1525 (1969).

16) W. Duffy, Jr., D. L. Strandburg, and J. F. Deck, *Phys., Rev.*, **183**, 567 (1969).

17) A. Kosaki, Y. Iida, M. Sorai, H. Suga, and S. Seki, *Bull. Chem. Soc. Jpn.*, **43**, 2280 (1970).

18) W. Duffy, Jr., J. F. Dubach, P. A. Pianetta, J. F. Deck, D. L. Strandburg, and A. R. Miedema, *J. Chem. Phys.*, **56**, 2555 (1972).

19) J. Yamauchi, K. Adachi, and Y. Deguchi, *Chem. Lett.*, **1972**, 733.

20) J. G. Vegter, T. Himba, and J. Kommandeur, *Chem. Phys. Lett.*, **3**, 427 (1969); J. G. Vegter and J. Kommandeur, *Mol. Cryst. Liq. Cryst.*, **30**, 11 (1975). These papers deal with the transition enthalpies of alkali-metal TCNQ salts by means of a differential scanning calorimeter.

21) A. Kosaki, M. Sorai, H. Suga, and S. Seki, *Bull. Chem. Soc. Jpn.*, **50**, 817 (1977).

22) Y. Matsunaga, *Can. J. Chem.*, **38**, 1172 (1960).

23) Y. Iida, *Bull. Chem. Soc. Jpn.*, **43**, 345 (1970).

24) A. Girlando, L. Morelli, and C. Pecile, *Chem. Phys. Lett.*, **22**, 553 (1973).

25) G. Scheibe, F. May, and H. Fischer, *Ber.*, **57**, 1330 (1924).

26) H. A. Torrey and W. H. Hunter, *J. Am. Chem. Soc.*, **34**, 702 (1912).

27) H. Suga and S. Seki, *Bull. Chem. Soc. Jpn.*, **38**, 1000 (1965).

28) J. W. Bray, H. R. Hart, Jr., L. V. Interrante, I. S. Jacobs, J. S. Kasper, G. D. Watkins, S. H. Wee, and J. S. Bonner, *Phys. Rev. Lett.*, **35**, 744 (1975).

29) E. Pytte, *Phys. Rev.*, *B*, **10**, 4637 (1974).

30) J. Frenkel, "Kinetic Theory of Liquids," Oxford University Press, London (1947), Chap. VII.